Kondo lattice effects and the collapse of lattice coherence in $Yb_{1-x}Lu_xB_{12}$ studied by hard x-ray photoelectron spectroscopy

J. Yamaguchi,[1] A. Sekiyama,[1] S. Imada,[1,*] H. Fujiwara,[1,†] M. Yano,[1] T. Miyamachi,[1] G. Funabashi,[1] M. Obara,[1] A. Higashiya,[2] K. Tamasaku,[2] M. Yabashi,[2,3] T. Ishikawa,[2,3] F. Iga,[4] T. Takabatake,[4] and S. Suga[1]

[1]*Graduate School of Engineering Science, Osaka University, Toyonaka, Osaka 560-8531, Japan*

[2]*RIKEN, Sayo, Hyogo 679-5148, Japan*

[3]*Japan Synchrotron Radiation Research Institute, Sayo, Hyogo 679-5198, Japan*

[4]*Graduate School of Advanced Sciences of Matter, Hiroshima University, Higashi-Hiroshima 739-8526, Japan*

(Received 24 December 2008; revised manuscript received 17 February 2009; published 30 March 2009)

Kondo semiconductor YbB_{12} and the Lu-substituted $Yb_{1-x}Lu_xB_{12}$ ($x=1/8$) alloy have been studied by the bulk-sensitive hard x-ray ($h\nu\sim 8$ keV) photoelectron spectroscopy at temperatures from 200 down to 20 K. To check the Kondo lattice effects for the bulk electronic states, the temperature dependence of the bulk Yb valence and $4f$ peak positions in both systems is analyzed with use of the single-impurity Anderson model (SIAM) by considering the crystalline electric field effects. For $x=0$, the temperature dependence of the bulk electronic states cannot be interpreted within the SIAM, whereas those for $x=1/8$ could be understood by the SIAM predictions due to the collapse of the lattice coherence by the Lu substitution. These results indicate that the Kondo lattice effects are important for pure YbB_{12} and play essential roles for forming a narrow gap at low temperatures.

DOI: 10.1103/PhysRevB.79.125121 PACS number(s): 79.60.−i, 75.20.Hr, 75.30.Mb

I. INTRODUCTION

Among strongly correlated electron systems containing rare-earth elements, CeNiSn,[1] $Ce_3Bi_4Pt_3$,[2] SmB_6,[3] and YbB_{12} (Refs. 4 and 5) have been well known as valence-fluctuating (VF) Kondo semiconductors (or Kondo insulators). They behave as metals or semimetals near the room temperature with localized $4f$ magnetic moments, whereas a nonmagnetic insulating ground state develops below a characteristic temperature (T^*) of the order of 100 K with opening a narrow energy gap (~10 meV) at the Fermi level (E_F). However, the mechanism of the gap formation is still controversial.

Among those compounds, YbB_{12} is regarded as a candidate material, where the mechanism of the narrow gap formation may be clarified because of its very simple NaCl-type crystal structure (with Yb cations in the sodium ion site and B_{12} dodecahedra in the chlorine ion site, forming the two interpenetrating fcc sublattices).[5] Thus, detailed studies of YbB_{12} can promote the understanding of physics in Kondo semiconductors. To date, many experimental and theoretical approaches have been performed for YbB_{12}. The magnetic susceptibility follows a Curie-Weiss behavior above 170 K. It shows a broad maximum around $T^*\sim 80$ K and then decreases rapidly to reach a constant value characterized by the nonmagnetic ground state.[6,7] The Kondo temperature (T_K) is conventionally estimated as $\sim 3T^*$, suggesting $T_K\sim 240$ K.[7] The narrow gap in YbB_{12} opens below 80 K. The gap magnitude at low temperatures has been estimated to be 11.7 meV from the electrical resistivity,[6] 15.5 meV from the Hall coefficient,[6] ~10 meV from the low photon energy ($h\nu=21.2$ eV) photoelectron spectroscopy (PES),[8] and 15 meV from the optical conductivity results.[9] In addition, local density approximation with the strong Coulomb U correlation (LDA+U) band-structure calculations considering the realistic orbital degeneracies in both conduction bands and $4f$ states have given the gap of ~17.7 meV.[10]

The Yb mean valence for YbB_{12} has been estimated from several spectroscopic techniques. The Yb valence is estimated as 2.86 ± 0.06 at 30 K and 2.9 at room temperature from the soft x-ray (SX) PESs at $h\nu=125$ eV (Ref. 11) and at $h\nu=1253.6$ eV (Mg $K\alpha$),[12] respectively. These techniques have, however, such experimental problems as the surface sensitivity due to the short inelastic mean-free path (IMFP: $\lambda\sim 6$ Å at $h\nu=125$ eV) (Ref. 13) of the photoelectrons and the insufficient energy resolution (1.1 eV at $h\nu=1253.6$ eV). As a bulk-sensitive technique, the Yb L_{III} ($2p_{3/2}$) edge x-ray absorption spectroscopy (XAS) has been performed and the Yb valence is estimated to be very close to 3 (larger than 2.95) at 20 K.[14] However, the valence evaluation from the Yb L_{III}-edge XAS spectra is rather limited because the Yb^{2+} and Yb^{3+} components strongly overlap and the separation into the two components has some ambiguities. Therefore, more accurate estimate of the bulk Yb valence is required to clarify the VF behavior in YbB_{12}.

In order to examine the evolution of the narrow gap, electronic properties of the Lu-substituted system $Yb_{1-x}Lu_xB_{12}$ have been studied. In the study of the x dependence of optical conductivity spectra,[15] the onset attributed to the gap in the optical spectrum for $x=0$ disappears rapidly by substituting a small amount of Lu ($x=1/8$). The gap filling for small x may imply the reduction of the Kondo lattice effects described by the periodic Anderson model (PAM).[16] Moreover, the importance of the Kondo lattice effects for YbB_{12} was also suggested in Ref. 17. On the other hand, in inelastic neutron-scattering (INS) studies of $Yb_{1-x}Lu_xB_{12}$,[18] the gap can be traced up to $x=0.9$ in INS spectra. Then it has been concluded that the gap could be driven by the Yb $4f$ single-site effects rather than the Kondo lattice effects. Therefore, detailed investigations of the bulk electronic states of $Yb_{1-x}Lu_xB_{12}$ are required to settle these controversies between optical and INS studies. So far, in many Yb-based VF compounds the competition between the Kondo lattice ver-

sus $4f$ single-site effects has been discussed as a key issue.[19–22]

This paper reports on bulk-sensitive hard x-ray PES (HAXPES) studies of Kondo semiconductor YbB_{12} and the Lu-substitution alloy $Yb_{7/8}Lu_{1/8}B_{12}$. The high energy PES has been widely recognized as one of the powerful tools to reveal bulk electronic states for strongly correlated electron systems.[23–26] First, the temperature (T) dependence of the bulk Yb valence has been estimated from the Yb $3d$ core-level spectra. Second, the T dependence of the bulk Yb valence and $4f$ peak positions in both systems is analyzed by the noncrossing approximation (NCA) calculation[27] based on the single-impurity Anderson model (SIAM) (Ref. 28) considering the crystalline electric field (CEF) effects. From a comparison between experimental and theoretical results, we discuss that Kondo lattice effects in pure YbB_{12} and the collapse of the lattice coherence induced by substituting a small amount of Lu for Yb.

II. EXPERIMENT

The single crystals of $Yb_{1-x}Lu_xB_{12}$ ($x=0$ and 1/8) were grown by the floating-zone method by using an image furnace with four xenon lamps.[6,7] These bulk properties are characterized by the electrical resistivity,[6] the magnetic susceptibility,[6,7] the heat capacity,[7] and the Hall coefficient[6] measurements. In accordance with the Lu substitution, the Kondo temperature conjectured from the shift of T^* in the magnetic susceptibility increases only slightly from $T_K \sim 240$ K for $x=0$ to $T_K \sim 250$ K for $x=1/8$.[7] On the other hand, the lattice constant is almost unchanged between $x=0$ and 1/8.[29]

HAXPES measurements were performed at the 27 m long undulator beam line 19LXU of SPring-8.[30] The x-ray radiation was monochromatized by Si(111) double crystals and then monochromatized by a Si(551) ($h\nu=8180$ eV for $x=0$) or a Si(444) ($h\nu=7942$ eV for $x=1/8$) channel-cut crystal. The spot size of the x ray focused with bimorph mirrors onto the sample was 100 μm (vertical) $\times$ 60 μm (horizontal). An MBS A1-HE spectrometer was employed for electron energy analyses. The samples were fractured *in situ* in a vacuum with a base pressure of better than 5×10^{-8} Pa. The measurements were performed at temperatures from 200 to 20 K. The surface cleanliness was confirmed by the absence of the O $1s$ and C $1s$ HAXPES signals. The energy calibration was performed by the Au Fermi edge at each measuring T. The total-energy resolution was set to 460 meV for Yb $3d$ core-level spectra, 120 meV for Yb $4f$ spectra in the wide energy region (−1–13.5 eV), and 65 meV for Yb^{2+} $4f_{7/2}$ spectra in the narrow energy region (−0.25–1.0 eV).

III. RESULTS AND DISCUSSION

A. Yb valence estimation from Yb 3*d* core-level spectra

The Yb $3d$ core-level HAXPES spectra of YbB_{12} and $Yb_{7/8}Lu_{1/8}B_{12}$ are given in Fig. 1(a). Characteristic features derived from the Yb^{2+} and Yb^{3+} states are observed in both spectra. The single peaks at 1520 and 1568 eV are due to the Yb^{2+} $3d_{5/2}$ and $3d_{3/2}$ states corresponding to the $3d^{10}4f^{14}$ initial state $\rightarrow 3d^9 4f^{14}$ final-state excitation. The Yb^{3+} $3d$ states ($3d^{10}4f^{13}$ initial state $\rightarrow 3d^9 4f^{13}$ final state) are observed as multiplet structures around 1527 eV for the $3d_{5/2}$ state and 1577 eV for the $3d_{3/2}$ state. For $x=1/8$, the Lu^{3+} $3d_{5/2}$ component ($3d^{10}4f^{14}$ initial state $\rightarrow 3d^9 4f^{14}$ final state) and its $3d_{3/2}$ spin-orbit partner are observed at 1589 and 1640 eV, respectively. In addition, broad satellites at 1550 and 1600 eV are due to the inelastic energy-loss structures, which are often observed in the $3d$ core-level spectra of rare-earth compounds.[31–33] The T-dependent Yb $3d_{5/2}$ spectra are shown in Fig. 1(b) for $x=0$ and in Fig. 1(c) for $x=1/8$. It is noticed in both systems that the Yb^{2+} $3d$ spectral weight is gradually increased on cooling from 200 down to 20 K due to the development of the Kondo resonance. Such an increase of the Yb^{2+} component for YbB_{12} with decreasing T has been observed in previous PES measurements.[34,35]

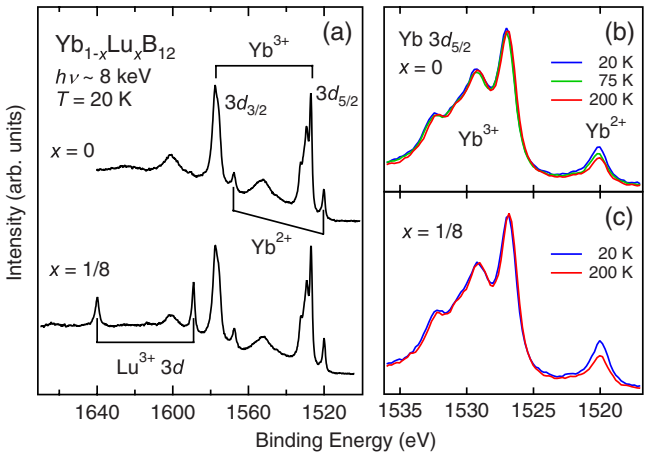

FIG. 1. (Color online) Yb $3d$ core-level spectra of $Yb_{1-x}Lu_xB_{12}$ ($x=0$ and 1/8) measured at $h\nu \sim 8$ keV. (a) Whole energy region of the Yb $3d$ states. Lu^{3+} $3d$ peaks are seen for $x=1/8$. T-dependent Yb $3d_{5/2}$ spectra (b) for $x=0$ and (c) for $x=1/8$. All spectra are normalized by the integrated intensity of the Yb^{3+} $3d$ multiplet structures.

In order to estimate the T dependence of the bulk Yb valence for $x=0$ and 1/8, we have carried out numerical fitting of the Yb $3d$ core-level spectra. The advantages of the valence estimation from the Yb $3d$ core-level spectra are as follows: (i) the bulk-sensitivity is high enough to suppress the contributions of the surface and subsurface layers due to the large IMFP ($\lambda \sim 90$ Å at $h\nu \sim 8$ keV), (ii) the Yb^{2+} and Yb^{3+} $3d$ components are well separated due to the large $3d$-$4f$ Coulomb attractive energy (~ 10 eV),[36] and (iii) other Auger lines do not appear in the Yd $3d$ core-level binding-energy (E_B) region. In the fitting procedure, the calculated PES line spectra are convoluted with the Lorentzian function for the lifetime broadening and the Gaussian function for the instrumental resolution [the full width at half maximum (FWHM) of the Gaussian Γ_G is assumed to be 460 meV]. The Mahan's asymmetry factor α (Ref. 37) and the FWHMs of the Lorentzian Γ_L were regarded as fitting parameters. These values are assumed as $\alpha=0.08$, $\Gamma_L \sim 1.3$ eV for the Yb $3d_{5/2}$ state, and $\Gamma_L \sim 1.9$ eV for the Yb $3d_{3/2}$ state. The different Γ_L values between the Yb $3d_{5/2}$ and $3d_{3/2}$ states are due to the E_B-dependent lifetime broadening.[38] The energy-

TABLE I. The electrostatic interaction values of Slater integral (F and G) and spin-orbit (ζ) parameters (in eV) for initial and final states in the $3d$ PES of the Yb trivalent ion. These values are reduced to 85%–98% by multiplying the HF calculation results with the reduction factor r_{HF}.

	Yb^{3+}	r_{HF}
$3d^{10}4f^{13}$		
ζ_f	0.366	0.98
$3d^{9}4f^{13}$		
$F^2(df)$	10.37	0.85
$F^4(df)$	4.95	0.85
$G^1(df)$	7.71	0.85
$G^3(df)$	4.53	0.85
$G^5(df)$	3.13	0.85
ζ_d	18.903	0.98
ζ_f	0.426	0.98

loss satellites are located at 23.4 eV from the respective main component and fitted with $\Gamma_L \sim 6.4$ eV. The multiplet structures of the Yb^{3+} $3d$ state were calculated by using the XTLS 8.0 program.[39] The values of electrostatic interaction parameters were obtained by the atomic Cowan's code[40] based on the Hartree-Fock (HF) method as shown in Table I. Each parameter is multiplied by the reduction factor r_{HF} to fit the experimental data.

As an example, the fitting result of the Yb $3d$ core-level spectrum for YbB_{12} is shown in Fig. 2. The line spectra show the calculated Yb^{3+} $3d$ multiplet structures. The whole spectrum is well reproduced by the fitting procedure described above. The bulk Yb valence can then be estimated from the integrated intensity ratio between the Yb^{2+} and Yb^{3+} components. For both $x=0$ and 1/8 systems, we have obtained the results of the T dependence of the Yb valence, as shown in

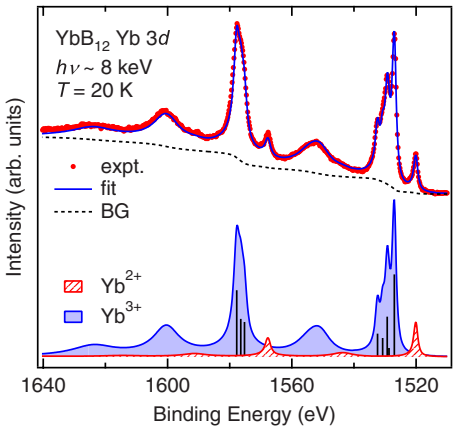

FIG. 2. (Color online) Numerical fitting to the Yb $3d$ core-level spectrum of YbB_{12}. In the upper panel, experimental data (red dots) and the fitting curve (blue solid line) are shown, and the integral-type background (BG) is indicated as a dashed line. Shaded and filled areas in the lower panel represent the calculated Yb^{2+} and Yb^{3+} $3d$ line shapes including their energy-loss satellites. Vertical bars are the line spectra of the calculated Yb^{3+} $3d$ multiplet, as described in the text.

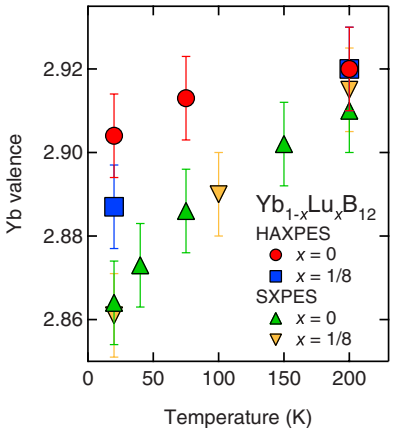

FIG. 3. (Color online) T dependence of the Yb valence estimated from the Yb $3d$ HAXPES ($h\nu \sim 8$ keV) and Yb $4f$ SXPES ($h\nu=700$ eV) (Ref. 41) spectra of $Yb_{1-x}Lu_xB_{12}$ ($x=0$ and 1/8).

Fig. 3. For comparisons, the Yb valences estimated from the Yb $4f$ SXPES spectra at $h\nu=700$ eV for $x=0$ and 1/8 are added in Fig. 3.[41] The values of the Yb valence show a gradual decrease on cooling from 200 down to 20 K in all cases. When we compare the Yb valence for $x=0$ to that for $x=1/8$ in both HAXPES and SXPES, we can see that the changes of the Yb valence by substituting a small amount of Lu are less than 0.02. On the other hand, one notices that the difference in the Yb valence between HAXPES and SXPES in both systems becomes larger with decreasing T, i.e., the Yb valence derived from SXPES is slightly closer to divalence compared to that derived from HAXPES. It is known that Yb ions in the surface layer are almost divalent and the subsurface layer has a more Yb^{2+}-rich property than the bulk.[42–44] This means that the contributions of the subsurface layer are not fully separated in the fitting procedure of the Yb $4f$ SXPES spectra.[41] Namely, some ambiguities remain on the spectral weight of subsurface components in the SXPES case of $Yb_{1-x}Lu_xB_{12}$. We have known that the thickness of the surface (d_s) plus subsurface (d_{ss}) layer is comparable to the lattice constant in some Yb-based VF compounds.[45] The spectral weights of the surface (W_s), subsurface (W_{ss}), and bulk (W_b) components are given by $W_s=1-\exp(-d_s/\lambda)$, $W_{ss}=\exp(-d_s/\lambda)-\exp[-(d_s+d_{ss})/\lambda]$, and $W_b=\exp[-(d_s+d_{ss})/\lambda]$. If we assume d_s+d_{ss} as the lattice constant ($a \sim 7.468$ Å) of YbB_{12} and $Yb_{7/8}Lu_{1/8}B_{12}$,[29] i.e., $d_s=2.0$ Å and $d_{ss}=5.5$ Å,[46] the relative spectral weights are $W_s:W_{ss}:W_b=0.02:0.06:0.92$ for HAXPES ($\lambda \sim 90$ Å) and $W_s:W_{ss}:W_b=0.12:0.27:0.61$ for SXPES ($\lambda \sim 15$ Å). Therefore, we conclude that the Yb valence estimated from the Yb $3d$ core-level HAXPES spectra is very close to the intrinsic bulk value.

B. Yb $4f$ peak positions in valence-band spectra

Figure 4 shows the valence-band HAXPES spectra of YbB_{12} and $Yb_{7/8}Lu_{1/8}B_{12}$ at 20 K. Corresponding Yb^{3+} $4f$ ($4f^{13}$ initial state $\rightarrow 4f^{12}$ final state) multiplet structures [shown by the line spectra for $x=0$ after proper energy scaling (~ 1.1) for the calculated atomic multiplet] (Ref. 47) are

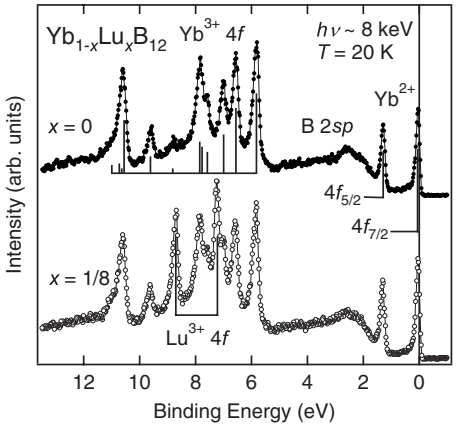

FIG. 4. Valence-band spectra of $Yb_{1-x}Lu_xB_{12}$ ($x=0$ and 1/8). For $x=0$, the calculated Yb^{3+} $4f$ multiplet structures (Ref. 47) are shown by line spectra. Spectra are normalized by the integrated intensity of the Yb^{3+} $4f$ multiplet structures.

present between 6 and 12 eV. Meanwhile two sharp peaks observed just below E_F and at 1.3 eV are derived from the Yb^{2+} $4f_{7/2}$ state ($4f^{14}$ initial state$\rightarrow 4f^{13}$ final state) and its spin-orbit partner $4f_{5/2}$ state, respectively. In valence-band SXPES spectra, broad peaks derived from the surface layer were reported in the Yb^{2+} $4f$ E_B region (1–2 eV).[8,11,35,41] These broad peaks are, however, suppressed in the HAXPES spectra owing to its high bulk sensitivity. For $x=1/8$, one can see the Lu^{3+} $4f$ doublet peaks ($4f^{14}$ initial state$\rightarrow 4f^{13}$ final state) overlapping with the Yb^{3+} $4f$ multiplet structures. The broad structures in 2–6 eV are almost unchanged by Lu substitution. Based on the band-structure calculations for YbB_{12} (Refs. 10, 48, and 49) and the photoionization cross sections,[50] such structures are expected to be dominated by the B $2s$ and $2p$ bonding states. The B_{12} dodecahedron molecules form rigid cages, resulting in the splitting of the B electronic states into the s-p bonding and antibonding states separated by a large gap crossing E_F. The B $2s$ and $2p$ bonding states correspond to the valence bands.[51]

In order to evaluate the T dependence of the accurate peak positions of the bulk Yb $4f$ spectra for $x=0$ and 1/8, the Yb $4f$ spectra have been fitted with the similar procedure, as mentioned before in Sec. III A. The fitting result of the Yb $4f$ spectrum for YbB_{12} is shown in Fig. 5(a). The intensity ratio between the Yb^{2+} and Yb^{3+} $4f$ peaks is determined by taking into account the Yb valence estimated from the Yb $3d$ core-level spectrum. Then, one can see that the redundant non-$4f$ valence bands overlap even with the Yb^{3+} $4f$ multiplet structures [see the dash-dot line in Fig. 5(a)]. The non-$4f$ bands are dominated by the above-mentioned B $2s$ and $2p$ bonding states.

The T dependence of the first peak ($^3H_6$) of the Yb^{3+} $4f$ multiplet structures and the Yb^{2+} $4f_{7/2}$ peak (the so-called Kondo resonance peak) is shown in Figs. 5(b)–5(e). The symbols (red squares for 200 K and blue circles for 20 K) and solid lines indicate the experimental data and the fitted curves. The T dependence of the peak positions in Figs. 5(b)–5(e) is summarized in Figs. 6(b) and 6(c). The Yb^{2+} $4f_{7/2}$ peak position for $x=0$ is found to be 56 meV at 200 K and 36 meV at 20 K as shown in Fig. 6(b). Namely, the peak

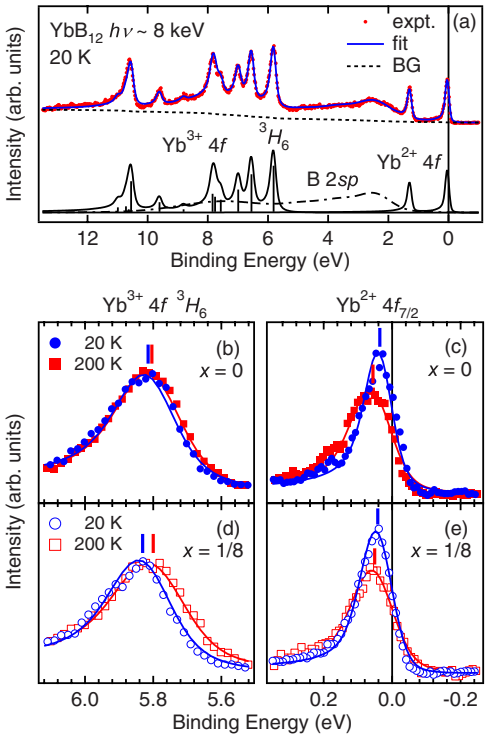

FIG. 5. (Color online) Numerical fitting to the Yb $4f$ valence-band spectrum of $Yb_{1-x}Lu_xB_{12}$. (a) Fitting result of the Yb $4f$ spectrum in the wide energy region for YbB_{12}. The broad B $2sp$ structure (dash-dot line) is fitted with several Gaussian and Lorentzian functions. (b) and (c) are the fitting results for the Yb^{3+} $4f$ $^3H_6$ peak and the Yb^{2+} $4f_{7/2}$ peak for $x=0$. (d) and (e) are ones for $x=1/8$. The fitting parameters are as follows: $\alpha=0.13$ for the Yb^{2+} and Yb^{3+} $4f$ states, $\Gamma_L \sim 120$ meV for the Yb^{3+} $4f$ multiplet structures, $\Gamma_L \sim 30$ meV for the Yb^{2+} $4f_{7/2}$ states. Γ_G is set to 120 meV for Yb $4f$ spectra in (a), (b), and (d). $\Gamma_G=65$ meV is employed for the Yb^{2+} $4f_{7/2}$ spectra in (c) and (e). Spectra in (b) and (d) are normalized by the integrated intensity of the Yb^{3+} $4f$ multiplet structures, and those in (c) and (e) are normalized by the integrated intensity of the Yb^{2+} $4f_{7/2}$ peak (−0.2–0.8 eV).

shift from 200 to 20 K is ~20 meV toward lower E_B side (the Yb^{2+} $4f_{5/2}$ peak shows the equivalent shift behavior). On the other hand, the $^3H_6$ peak (and also the whole peaks of the Yb^{3+} $4f$ multiplet structures) for $x=0$ is found to shift only slightly toward higher E_B side with decreasing T from 200 to 20 K, i.e., the center of gravity (COG) of the Yb^{3+} $4f$ multiplet structures is 7.758 eV at 200 K and 7.769 eV at 20 K [see Fig. 6(c)] and thus the peak shift is at most ~10 meV toward higher E_B side. These peak shifts of the Yb $4f$ spectra with T in HAXPES are quite different from our previous SXPES results for $x=0$.[41] This indicates that the contributions of the subsurface layer affect the Yb $4f$ peak shifts for SXPES in the case of YbB_{12}. This T dependence of the Yb $4f$ spectra in YbB_{12} for HAXPES is similar to that in dense Kondo metal $YbAl_3$, which is essentially governed by the Kondo lattice effects.[52] In contrast, the peak position of the Yb^{2+} $4f_{7/2}$ spectra for $x=1/8$ is found to be 51 meV at 200 K and 42 meV at 20 K. Namely, the peak shift is at most ~10 meV toward lower E_B side. Meanwhile the COG of the Yb^{3+} $4f$ multiplet structures is 7.754 eV at 200 K and 7.785

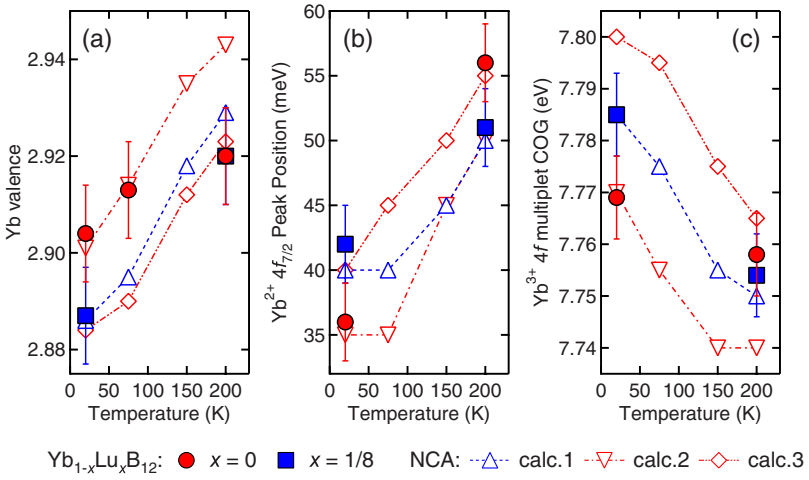

FIG. 6. (Color online) Comparison between experimental and NCA calculation results on the T dependence of (a) the Yb valence, (b) the Yb^{2+} $4f_{7/2}$ peak positions, and (c) the COG of the Yb^{3+} $4f$ multiplet structures.

eV at 20 K and thus the peak shift is ~30 meV toward higher E_B side with decreasing T.

C. NCA analyses based on SIAM

For quantitative discussions on the effects of small Lu substitution to the T dependence of the bulk Yb valence and $4f$ peak positions in $Yb_{1-x}Lu_xB_{12}$, we have carried out the NCA calculation based on SIAM. The NCA analyses have so far been applied to many Ce- and Yb-based compounds. In this calculation, the $4f^{14}$, $4f^{13}$ ($J=7/2$ and 5/2), and $4f^{12}$ states are considered as the initial states. Here, the CEF splitting of the $4f^{13}_{7/2}$ state is taken into account. The degeneracy of the $4f$ Γ_8, $4f$ Γ_7, $4f$ Γ_6, $4f^{13}_{5/2}$, and $4f^{12}$ states are considered as 4, 2, 2, 6, and 91, respectively. The CEF splitting energies Δ_{CEF87} (the energy difference between the $4f$ Γ_8 and Γ_7 states) and Δ_{CEF86} (one between the $4f$ Γ_8 and Γ_6 states) are derived from the INS estimation.[18] Their values are $\Delta_{CEF87}=70$ K and $\Delta_{CEF86}=130$ K and assumed to be the same for $x=0$ and 1/8. The spin-orbit splitting energy of the $4f^{13}$ states (the energy difference between the COG of the $4f^{13}_{7/2}$ and $4f^{13}_{5/2}$ states) is 1.25 eV. From the band-structure calculations for YbB_{12},[10] the Yb $4f$ states are mainly mixing with the conduction band with the Yb $5d$ t_{2g} character, which is lying within the band gap between bonding and antibonding bands resulting from the B $2s$-$2p$ states. Thus, the hybridization of the $4f$ states with a trapezoidal conduction band [which has the flat density of state (DOS) within ±1.5 eV from E_F and then the DOS becomes zero at ±2 eV] is assumed. The calculated $4f$ spectral functions are convoluted with the Fermi-Dirac function and the Gaussian function ($\Gamma_G=65$ meV) for the instrumental resolution. Other SIAM parameters to be optimized are as follows: (i) the bare $4f$ level ε_f (which is negative and corresponds to E_B of the $4f$ electrons in the $4f^{14}\rightarrow 4f^{13}$ process), (ii) the Coulomb repulsion energy U_{ff} between $4f$ electrons on the same site (E_B in the $4f^{13}\rightarrow 4f^{12}$ process is represented by ε_f+U_{ff}), and (iii) the averaged hybridization strength $\Delta=(\pi/2B)\int_{-B}^{B}\rho V^2(E)dE$ [where $\rho V^2(E)$ is the energy-dependent hybridization strength and B is the half of the conduction-band width ($B=2$ eV)].

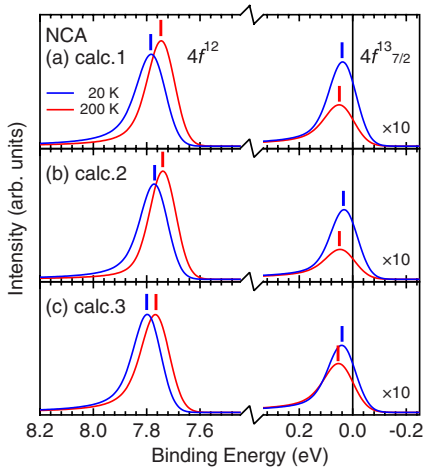

FIG. 7. (Color online) NCA spectra calculated with the SIAM parameter sets listed in Table II. All spectra have been normalized by the integrated intensity of the $4f^{12}$ peak.

Figures 7(a)–7(c) show the NCA spectra at 200 and 20 K calculated with the SIAM parameter sets listed in Table II. Here, the $4f^{12}$ multiplet structures are represented by a single component, whose intensity and peak position correspond to the integrated intensity and the COG of the whole $4f^{12}$ multiplet structures. As shown in Fig. 7(a), the NCA spectra calculated with the parameter set of calc.1 can reproduce the T dependence of the Yb $4f$ peak positions for $x=1/8$. The $4f^{13}_{7/2}$ peak position gradually shifts from 50 to 40 meV with decreasing T from 200 to 20 K, namely, the predicted peak

TABLE II. Optimized SIAM parameter sets for $Yb_{1-x}Lu_xB_{12}$ ($x=0$ and 1/8). The parameter sets of calc.1, calc.2, and calc.3 are used to reproduce experimental results for $x=1/8$, $x=0$ at 20 K, and $x=0$ at 200 K, respectively. T_K^{NCA}'s obtained from the NCA calculation are also given.

	ε_f (eV)	U_{ff} (eV)	Δ (meV)	T_K^{NCA} (K)
Calc.1	−0.910	8.52	63.8	~420
Calc.2	−0.915	8.53	60.8	~350
Calc.3	−0.955	8.58	68.4	~480

shift is 10 meV toward lower E_B side. On the other hand, the COG of the $4f^{12}$ multiplet structures shifts from 7.750 eV at 200 K to 7.785 eV at 20 K. Thus, the predicted peak shift is 35 meV toward higher E_B side on cooling. The calculated Yb valence with the parameter set of calc.1 gradually decreases from ~2.93 at 200 K to ~2.87 at 20 K. In Fig. 6, the comparisons between experimental results (full symbols) and NCA calculation results (empty symbols) on the T dependence are shown. For $x=1/8$, the NCA results (triangles △) are in rough agreement with the experimental T dependence (squares ■) evaluated from the bulk Yb $3d$ and $4f$ HAXPES spectra. In Lu-substituted dense Kondo metal $Yb_{0.6}Lu_{0.4}Al_3$, we have also confirmed that the detailed T dependence of the Yb $4f$ spectra is well understood within the SIAM.[53] In addition, we have confirmed that the T dependence for $x=1/8$ cannot be sufficiently reproduced if the CEF splitting is not taken into account in the calculations. If the CEF splittings were neglected, the $4f^{12}$ peak shifts from 200 to 20 K are overestimated as 50–60 meV (data not shown).[54] Thus, the CEF effects must be properly taken into account to discuss the bulk electronic states in $Yb_{1-x}Lu_xB_{12}$, since T_K's are not remarkably larger than Δ_{CEF87} and Δ_{CEF86}.

For $x=0$, the NCA spectra are likewise calculated with the parameter sets of calc.2 and calc.3 as shown in Figs. 7(b) and 7(c), respectively. The parameter set of calc.2 is determined to reproduce the Yb valence and $4f$ peak positions for $x=0$ at 20 K. In the calculation with this parameter set, the Yb valence and the $4f^{12}$ peak shift are overestimated with increasing T from 20 to 200 K compared to the experimental results [see triangles ▽ in comparison with circles ● in Figs. 6(a) and 6(c)]. In order to reproduce the Yb valence and $4f$ peak positions for $x=0$ at 200 K, different parameter sets of calc.3 must be employed. Although the Yb valence and the Yb^{2+} $4f_{7/2}$ peak position at 200 K are reproduced, the COG of the $4f^{12}$ multiplets is near the upper error bar limit [see diamonds ◇ in Fig. 6(c)]. In addition, the Yb valence and the Yb^{3+} $4f$ peak positions for $x=0$ at 20 K are not reproduced with the parameter set of calc.3 at all. It is already found from the NCA analyses with considering the CEF splitting that the T dependence of the Yb valence and $4f$ peak positions for $x=1/8$ could be explained within the SIAM with ignoring the influence of the $4f$ lattice periodicity. However, this treatment is found to be not applicable to $x=0$. Therefore, we conclude that the Kondo lattice effects are important for describing the bulk electronic states for pure YbB_{12}, to which the SIAM is not applicable. In our previous SXPES results for $x=0$,[41] the T dependence of the Yb valence and $4f$ peak positions was understood by the SIAM, which was similar to the present HAXPES results for $x=1/8$. The contributions of the subsurface layer in $Yb_{1-x}Lu_xB_{12}$ cannot be fully ignored in SXPES as mentioned before. Although the lattice coherence exists along the in-plane direction in the subsurface layer, that along the out-of-plane direction is broken. Then the T dependence of the Yb $4f$ SXPES spectra for $x=0$ may be governed by the Yb single-site effects and thus the SIAM might have been applicable. However, in the bulk probed by HAXPES, the inadequacy of the SIAM is confirmed. From our HAXPES results, it is difficult to discuss the details of the narrow gap formation in $Yb_{1-x}Lu_xB_{12}$ because of the insufficient instrumental resolution. However, in accordance with the present NCA analyses of the HAXPES spectra for $x=0$ and 1/8 and the gap filling observed in the optical conductivity spectrum for $x=1/8$,[15] we think that the Kondo lattice effects play an essential role in the narrow gap formation at low temperatures for pure YbB_{12}.

Finally, we briefly comment on the Kondo temperatures in $Yb_{1-x}Lu_xB_{12}$. The Kondo temperatures can be estimated by the NCA calculation (see T_K^{NCA}'s in Table II). When we compare T_K^{NCA}'s to T_K's expected from a relation of $T_K \sim 3T^*$ ($T_K \sim 240$ K for $x=0$ and $T_K \sim 250$ K for $x=1/8$), we notice that T_K^{NCA}'s are much lager than these T_K's, even in the case of $T_K^{NCA} \sim 420$ K calculated with the parameter set of calc.1 for $x=1/8$. A relation $T_K \sim 3T^*$ has been advocated for Ce- and Yb-based Kondo *metal* systems,[55] whereas it has been conventionally applied to Kondo semiconductors. Thus, the discrepancy between our T_K^{NCA}'s and T_K's would imply that in Kondo semiconductors and their dilute impurity substitution alloys, the above simple description may need proper modifications with the consideration of the band renormalization due to the narrow gap formation at low temperatures.

IV. CONCLUSION

In conclusion, the detailed T dependence of the Yb valence and $4f$ peak positions for the bulk electronic states in $Yb_{1-x}Lu_xB_{12}$ ($x=0$ and 1/8) has been investigated by HAXPES. The T dependence of the bulk Yb $4f$ spectra depends noticeably on substitution of a small amount of Lu, although the changes of the bulk Yb valence are small. From the NCA analyses taking account of the CEF splitting, it is confirmed that the T dependence of the Yb valence and $4f$ peaks for $x=1/8$ could be reproduced within the framework of the SIAM, whereas that for $x=0$ deviates much from the SIAM predictions. It follows from these results that the Kondo lattice effects are essential in pure YbB_{12} and the lattice coherence is significantly sensitive to the randomness of Yb sites. The concrete descriptions about the T dependence of the bulk electronic states and the Kondo temperature in pure YbB_{12} should be performed by using the PAM and/or a more realistic model. In future works, the narrow gap formation in $Yb_{1-x}Lu_xB_{12}$ will be investigated by using the ultrahigh-resolution extremely low energy photoelectron spectroscopy ($h\nu < 10$ eV).[56]

ACKNOWLEDGMENTS

We would like to thank Y. Nakatsu and S. Itoda for supporting experiments. The soft x-ray experiments were performed at the BL25SU in the SPring-8 with the approval of the Japan Synchrotron Radiation Research Institute (Proposal Nos. 2002A0433 and 2006B1722). Financial support was provided by the Grant-in-Aid for Science Research (Contract Nos. 18104007, 18684015, and Innovative Areas "Heavy Electrons" No. 20102003) of MEXT, Japan, the Global COE program (G10) of JSPS, Japan, and the Asahi Glass Foundation.

*Present address: College of Science and Engineering, Ritsumeikan University, Kusatsu, Shiga 525-8577, Japan.
†Present address: II Physikalisches Institut, Universität zu Köln, D-50937 Köln, Germany.

[1] M. F. Hundley, P. C. Canfield, J. D. Thompson, Z. Fisk, and J. M. Lawrence, Phys. Rev. B **42**, 6842 (1990).
[2] T. Takabatake, F. Teshima, H. Fujii, S. Nishigori, T. Suzuki, T. Fujita, Y. Yamaguchi, J. Sakurai, and D. Jaccard, Phys. Rev. B **41**, 9607 (1990).
[3] A. Menth, E. Buehler, and T. H. Geballe, Phys. Rev. Lett. **22**, 295 (1969).
[4] M. Kasaya, F. Iga, K. Negishi, S. Nakai, and T. Kasuya, J. Magn. Magn. Mater. **31-34**, 437 (1983).
[5] M. Kasaya, F. Iga, M. Takigawa, and T. Kasuya, J. Magn. Magn. Mater. **47-48**, 429 (1985).
[6] F. Iga, N. Shimizu, and T. Takabatake, J. Magn. Magn. Mater. **177-181**, 337 (1998).
[7] F. Iga, S. Hiura, J. Klijn, N. Shimizu, T. Takabatake, M. Ito, Y. Matsumoto, F. Masaki, T. Suzuki, and T. Fujita, Physica B **259-261**, 312 (1999).
[8] T. Susaki, Y. Takeda, M. Arita, K. Mamiya, A. Fujimori, K. Shimada, H. Namatame, M. Taniguchi, N. Shimizu, F. Iga, and T. Takabatake, Phys. Rev. Lett. **82**, 992 (1999).
[9] H. Okamura, T. Michizawa, T. Nanba, S. Kimura, F. Iga, and T. Takabatake, J. Phys. Soc. Jpn. **74**, 1954 (2005).
[10] T. Saso and H. Harima, J. Phys. Soc. Jpn. **72**, 1131 (2003).
[11] T. Susaki, A. Sekiyama, K. Kobayashi, T. Mizokawa, A. Fujimori, M. Tsunekawa, T. Muro, T. Matsushita, S. Suga, H. Ishii, T. Hanyu, A. Kimura, H. Namatame, M. Taniguchi, T. Miyahara, F. Iga, M. Kasaya, and H. Harima, Phys. Rev. Lett. **77**, 4269 (1996).
[12] F. Iga, Y. Takakuwa, T. Takahashi, M. Kasaya, T. Kasuya, and T. Sagawa, Solid State Commun. **50**, 903 (1984).
[13] S. Tanuma, C. J. Powell, and D. R. Penn, Surf. Interface Anal. **35**, 268 (2003).
[14] P. A. Alekseev, E. V. Nefeodova, U. Staub, J.-M. Mignot, V. N. Lazukov, I. P. Sadikov, L. Soderholm, S. R. Wassermann, Yu. B. Paderno, N. Yu. Shitsevalova, and A. Murani, Phys. Rev. B **63**, 064411 (2001).
[15] H. Okamura, M. Matsunami, T. Inaoka, T. Nanba, S. Kimura, F. Iga, S. Hiura, J. Klijn, and T. Takabatake, Phys. Rev. B **62**, R13265 (2000).
[16] H. Tsunetsugu, M. Sigrist, and K. Ueda, Rev. Mod. Phys. **69**, 809 (1997) and references cited therein.
[17] J. J. Joyce and A. J. Arko, Phys. Rev. Lett. **78**, 1831 (1997).
[18] P. A. Alekseev, J.-M. Mignot, K. S. Nemkovski, E. V. Nefeodova, N. Yu. Shitsevalova, Yu. B. Paderno, R. I. Bewley, R. S. Eccleston, E. S. Clementyev, V. N. Lazukov, I. P. Sadikov, and N. N. Tiden, J. Phys.: Condens. Matter **16**, 2631 (2004).
[19] S. J. Oh, S. Suga, A. Kakizaki, M. Taniguchi, T. Ishii, J. S. Kang, J. W. Allen, O. Gunnarsson, N. E. Christensen, A. Fujimori, T. Suzuki, T. Kasuya, T. Miyahara, H. Kato, K. Schonhammer, M. S. Torikachvili, and M. B. Maple, Phys. Rev. B **37**, 2861 (1988).
[20] D. P. Moore, J. J. Joyce, A. J. Arko, J. L. Sarrao, L. Morales, H. Hochst, and Y. D. Chuang, Phys. Rev. B **62**, 16492 (2000).
[21] J. M. Lawrence, P. S. Riseborough, C. H. Booth, J. L. Sarrao, J. D. Thompson, and R. Osborn, Phys. Rev. B **63**, 054427 (2001).
[22] S. Danzenbächer, Yu. Kucherenko, C. Laubschat, D. V. Vyalikh, Z. Hossain, C. Geibel, X. J. Zhou, W. L. Yang, N. Mannella, Z. Hussain, Z.-X. Shen, and S. L. Molodtsov, Phys. Rev. Lett. **96**, 106402 (2006).
[23] A. Sekiyama, T. Iwasaki, K. Matsuda, Y. Saitoh, Y. Ōnuki, and S. Suga, Nature (London) **403**, 396 (2000).
[24] S. Suga, Appl. Phys. A: Mater. Sci. Process. **92**, 479 (2008).
[25] A. Yamasaki, S. Imada, H. Higashimichi, H. Fujiwara, T. Saita, T. Miyamachi, A. Sekiyama, H. Sugawara, D. Kikuchi, H. Sato, A. Higashiya, M. Yabashi, K. Tamasaku, D. Miwa, T. Ishikawa, and S. Suga, Phys. Rev. Lett. **98**, 156402 (2007).
[26] M. Yano, A. Sekiyama, H. Fujiwara, Y. Amano, S. Imada, T. Muro, M. Yabashi, K. Tamasaku, A. Higashiya, T. Ishikawa, Y. Ōnuki, and S. Suga, Phys. Rev. B **77**, 035118 (2008).
[27] Y. Kuramoto, Z. Phys. B: Condens. Matter **53**, 37 (1983).
[28] O. Gunnarsson and K. Schonhammer, Phys. Rev. Lett. **50**, 604 (1983); Phys. Rev. B **28**, 4315 (1983).
[29] F. Iga, M. Kasaya, and T. Kasuya, J. Magn. Magn. Mater. **52**, 279 (1985).
[30] M. Yabashi, K. Tamasaku, and T. Ishikawa, Phys. Rev. Lett. **87**, 140801 (2001).
[31] H. Sato, K. Shimada, M. Arita, K. Hiraoka, K. Kojima, Y. Takeda, K. Yoshikawa, M. Sawada, M. Nakatake, H. Namatame, M. Taniguchi, Y. Takata, E. Ikenaga, S. Shin, K. Kobayashi, K. Tamasaku, Y. Nishino, D. Miwa, M. Yabashi, and T. Ishikawa, Phys. Rev. Lett. **93**, 246404 (2004).
[32] L. Moreschini, C. Dallera, J. J. Joyce, J. L. Sarrao, E. D. Bauer, V. Fritsch, S. Bobev, E. Carpene, S. Huotari, G. Vanko, G. Monaco, P. Lacovig, G. Panaccione, A. Fondacaro, G. Paolicelli, P. Torelli, and M. Grioni, Phys. Rev. B **75**, 035113 (2007).
[33] K.-H. Park and S.-J. Oh, Phys. Rev. B **48**, 14833 (1993).
[34] Y. Takeda, M. Arita, M. Higashiguchi, K. Shimada, M. Sawada, H. Sato, M. Nakatake, H. Namatame, M. Taniguchi, F. Iga, T. Takabatake, K. Takata, E. Ikenaga, M. Yabashi, D. Miwa, Y. Nishino, K. Tamasaku, T. Ishikawa, S. Shin, and K. Kobayashi, Physica B **351**, 286 (2004).
[35] Y. Takeda, M. Arita, M. Higashiguchi, K. Shimada, H. Namatame, M. Taniguchi, F. Iga, and T. Takabatake, Phys. Rev. B **73**, 033202 (2006).
[36] L. Degiorgi, T. Greber, F. Hullinger, R. Monnier, L. Schlapbach, and B. T. Thole, Europhys. Lett. **4**, 755 (1987).
[37] G. D. Mahan, Phys. Rev. B **11**, 4814 (1975).
[38] H. Ogasawara, A. Kotani, and B. T. Thole, Phys. Rev. B **50**, 12332 (1994).
[39] A. Tanaka, T. Jo, and G. A. Sawatzky, J. Phys. Soc. Jpn. **61**, 2636 (1992).
[40] R. D. Cowan, *The Theory of Atomic Structure and Spectra* (University of California Press, Berkeley, 1981).
[41] A. Shigemoto, J. Yamaguchi, A. Sekiyama, S. Imada, A. Yamasaki, A. Irizawa, T. Ukawa, T. Muro, F. Iga, T. Takabatake, and S. Suga, J. Electron Spectrosc. Relat. Phenom. **156-158**, 472 (2007).
[42] H. Sato, K. Yoshikawa, K. Hiraoka, M. Arita, K. Fujimoto, K. Kojima, T. Muro, Y. Saitoh, A. Sekiyama, S. Suga, and M. Taniguchi, Phys. Rev. B **69**, 165101 (2004).
[43] L. H. Tjeng, S.-J. Oh, E.-J. Cho, H.-J. Lin, C. T. Chen, G.-H. Gweon, J.-H. Park, J. W. Allen, T. Suzuki, M. S. Makivic, and D. L. Cox, Phys. Rev. Lett. **71**, 1419 (1993).
[44] T. Okane, S.-I. Fujimori, A. Ino, A. Fujimori, S. K. Dhar, C. Mitra, P. Manfrinetti, A. Palenzona, and O. Sakai, Phys. Rev. B **65**, 125102 (2002).
[45] $YbInCu_4$: S. Suga, A. Sekiyama, S. Imada, J. Yamaguchi, A. Shigemoto, A. Irizawa, K. Yoshimura, M. Yabashi, K.

Tamasaku, A. Higashiya, and T. Ishikawa (unpublished); $YbCu_2Si_2$: J. Yamaguchi, A. Sekiyama, H. Fujiwara, G. Funabashi, Y. Ōnuki, and S. Suga (unpublished).

[46] If the fracture surface is the (001) plane, d_s=2.0 Å approximately corresponds to the Yb one monolayer and d_{ss}=5.5 Å contains the second and the third Yb layers.

[47] F. Gerken, J. Phys. F: Met. Phys. **13**, 703 (1983).

[48] A. Yanase and H. Harima, Prog. Theor. Phys. **108**, 19 (1992).

[49] V. N. Antonov, B. N. Harmon, and A. N. Yaresko, Phys. Rev. B **66**, 165209 (2002).

[50] J. J. Yeh and I. Lindau, At. Data Nucl. Data Tables **32**, 1 (1985).

[51] T. Kasuya, Europhys. Lett. **26**, 277 (1994).

[52] S. Suga, A. Sekiyama, S. Imada, A. Shigemoto, A. Yamasaki, M. Tsunekawa, C. Dallera, L. Braicovich, T.-L. Lee, O. Sakai, T. Ebihara, and Y. Ōnuki, J. Phys. Soc. Jpn. **74**, 2880 (2005).

[53] J. Yamaguchi, A. Sekiyama, S. Imada, A. Yamasaki, M. Tsunekawa, T. Muro, T. Ebihara, Y. Ōnuki, and S. Suga, New J. Phys. **9**, 317 (2007).

[54] However, in high T_K ($\sim$1000 K) system $Yb_{0.6}Lu_{0.4}Al_3$, the T dependence of the Yb 4f spectra is well reproduced by the SIAM, even if the CEF splittings ($\lesssim$120 K) were ignored (Ref. 53).

[55] N. E. Bickers, D. L. Cox, and J. W. Wilkins, Phys. Rev. Lett. **54**, 230 (1985).

[56] G. Funabashi, H. Fujiwara, A. Sekiyama, M. Hasumoto, T. Ito, S. Kimura, P. Baltzer, and S. Suga, Jpn. J. Appl. Phys. **47**, 2265 (2008).